Available online at www.sciencedirect.com
ScienceDirect
Ceramics International 35 (2009) 2531–2535
CERAMICS INTERNATIONAL
www.elsevier.com/locate/ceramint

Short communication

Mössbauer effect study of the Fe-substituted NASICON

A. Ignaszak [a,*], S. Komornicki [b], P. Pasierb [b]

[a] The University of British Columbia, Department of Chemical and Biological Engineering, 2360 East Mall, Vancouver BC V6T 1Z3, Canada
[b] AGH University of Science and Technology, Faculty of Materials Science and Ceramics, Department of Inorganic Chemistry, al. Mickiewicza 30, 30-059 Krakow, Poland

Received 12 May 2008; received in revised form 2 January 2009; accepted 4 February 2009
Available online 25 February 2009

Abstract

Fe-substituted NASICON was prepared by co-precipitation method and the content of iron at different oxidation states was estimated by Mössbauer spectroscopy (MS). Compounds with different phase composition were obtained depending on the preparation procedure. In the case of samples sintered in reducing atmosphere, NASICON containing di- and trivalent iron was detected. The lattice constants were calculated by Rietveld method. Higher values of the unit cell parameters for $Na_3Zr_{1-y}Fe_{1-y}^{2+}Fe_{2y}^{3+}P_3O_{12}$ compared to the structural analogue γ-$Na_3Fe_2P_3O_{12}$ indicated the partial replacement of smaller Fe^{3+} ions by bigger Fe^{2+} and Zr^{4+} in the NASICON lattice. The validation of Mössbauer spectroscopy as the useful tool in the calculation of iron content was also performed. The sintering in air led to the multiphase product, which was identified by XRD and MS.

Keywords: NASICON; X-ray diffraction; Mössbauer spectroscopy

1. Introduction

NASICON (Na^+ Super Ionic Conductor) is a name of compounds showing high ionic conductivity. These materials have been proposed for use as the solid electrolyte in solid-state electrochemical devices such as gas sensors, ion sensors and Na-S batteries [1–3].

The structure of NASICON is described by the general formula $AMM'P_3O_{12}$, where A can be alkali ions and M, M′ can be tri-, tetra- and pentavalent ions. A ions are located in two sites. In type I, A ions are sandwiched between two MO_6 (or $M'O_6$) octahedra along the *c* axis giving rise to disorder octahedral coordination. In II type, the A sites are perpendicular to the *c* axis with trigonal prismatic coordination. The structure is characterised as the 3-dimensional network of MO_6 (or $M'O_6$) octahedra, sharing corners with PO_4 tetrahedra and forming tunnels which may be vacant, partially or full occupied by A ions. Ionic conduction takes place when A ions move from one site to another through ''bottleneck'' formed by oxygen ions [4]. The complicated electronic and crystallographic structures of NASICON, as well as a doping in cationic and anionic sublattices give many possibilities of modification of its electrical properties. The doping by transition metals such as Fe, Nb, Ti, V or Cr improves an ionic conductivity and generates electronic component. It was supposed that the introduction of Fe^{2+} and Fe^{3+} into a lattice, results in a mixed conductivity, thus making possible to use it as the electrode material [5–7]. All NASICONs containing iron crystallise in rhombohedral structure and are isostructural with γ-$Na_3Fe_2P_3O_{12}$ [6–7]. Homogenous solid solution $Na_3Zr_{1-y}Fe_{1-y}^{2+}Fe_{2y}^{3+}P_3O_{12}$ was obtained for $0 < y < 0.5$ by solid-state reaction. The investigations of unit cell parameters showed the decrease of lattice constants with increasing iron content (y), as the result of the partial replacement of bigger Zr^{4+} ($r_{Zr^{4+}} = 0.079$ nm) and Fe^{2+} ($r_{Fe^{2+}} = 0.074$ nm) ions by two smaller Fe^{3+} ($r_{Fe^{3+}} = 0.064$ nm) [5]. The best electrical conductivity at 300 °C with similar ionic and electronic components was found for the composition of $y = 0.33$ in $Na_3Zr_{1-y}Fe_{1-y}^{2+}Fe_{2y}^{3+}P_3O_{12}$. This system will be subjected in our work.

Mössbauer spectroscopy has been used to investigate the oxidation states and the iron coordination in NASICON-type NASICON e.g. $Li_3Fe_2P_3O_{12}$ [6] or $NbTiP_3O_{12}$ [8]. For the sample containing only Fe^{3+} ($Li_3Fe_2P_3O_{12}$) Mössbauer spectra

* Corresponding author. Tel.: +1 604 827 3419; fax: +1 604 822 6003.
E-mail addresses: aignaszak@chml.ubc.ca, aignaszak@gmail.com (A. Ignaszak).

0272-8842/$34.00
doi:10.1016/j.ceramint.2009.02.003

showed a very narrow doublet with small quadrupolar splitting. As the Fe^{2+} increased two doubles appeared assigned to trivalent and divalent iron [6]. The values of isomer shift and quadrupolar splitting, characteristic for Fe^{3+} in high-spin octahedral configuration were detected in $Ca_{0.5}NbFeP_3O_{12}$ [7]. The large quadruple splitting corresponding to Fe^{2+} and Fe^{3+} was observed in Mössbauer spectrum for its reduced product $Ca_{0.5}NbFe_{1-x}Fe_xP_3O_{12}$. In addition, the value of isomer shift was typical for divalent iron in high spin octahedral coordination [7]. Barry et al. observed the change in intensities on the Mössbauer spectra depending on phase composition [8]. Mössbauer parameters, representative for Fe^{2+} were estimated for single-phase $Fe_{0.33}NbTiP_3O_{12}$. In comparison, Mössbauer spectra taken for the same sample after sintering in air showed additional patterns, typical for octahedrically coordinated Fe^{3+} in hematite phase, together with doublets corresponding to divalent iron existing in the main product ($Fe_{0.33}NbTiP_3O_{12}$). The variation of Fe^{2+} and Fe^{3+} intensities on Mössbauer spectra depending on heat treatment was also discussed [8].

In this work, we have applied Mössbauer spectroscopy in order to estimate the presence and content of iron at different oxidation states in NASICON synthesized by co-precipitation method. The phase identification and calculations of the unit cell parameters were obtained from X-ray diffraction. All results are compared with NASICON containing only Fe^{3+} ions and referred to the literature data for similar compounds. Mössbauer spectroscopy is applied for the first time to investigate metal incorporation into $Na_3Zr_{1-y}Fe_{1-y}{}^{2+}Fe_{2y}{}^{3+}P_3O_{12}$ framework.

2. Materials and methods

$Na_3Zr_{1-y}Fe_{1-y}{}^{2+}Fe_{2y}{}^{3+}P_3O_{12}$ for $y = 0.33$ was prepared by co-precipitation method from aqueous solutions of NaOH (POCh, Poland), $(NH_4)_2HPO_4$ (Aldrich), $ZrO(NO_3)_2$ (0.1205 g ZrO_2 in 1 g of solution), $Fe(NO_3)_3{\cdot}9H_2O$ (0.0796 g in 1 g of solution) (Aldrich), which were mixed in stoichiometric amount, assuming Zr/Fe (1/2) molar ratio. All reagents were stirred to form a gel-like solid bulk. Precipitate was dried at 150 °C, calcined at 700 °C for 24 h and grinded in 2-propanol for 5 h using zirconia grinding balls. The dried material was formed into discs with 13 mm diameter and pressed isostatically at 300 MPa. In order to obtain different materials, the one containing only Fe^{3+} (sample A) and the other containing both Fe^{3+}/Fe^{2+} ions (sample B), sintering was performed at different oxygen partial pressure, at the same temperature (850 °C) and time (3 h). Sample A was sintered in air and sample B at $pO_2 \cong 10^{-13}$ Pa. In order to estimate the stability of sample B, material was investigated by thermogravimetry in air (data not shown). The significant mass increase above 600 °C (followed by the surface oxidation at 360 °C) and red color of sample after TGA experiment showed formation of the multiphase product with a similar composition (identified by XRD) like sample A.

X-ray diffraction (X'Pert Philips) was applied for the phase identification. Unit cell parameters were calculated by Rietveld method from measured XRD patterns in 2Θ range of 10–130° (0.008° step and 200 s). X'Pert Plus software coupled with X'Pert MRD Philips instrument was used for data analysis. All measurements were carried out at room temperature.

The Mössbauer effect measurements were performed at room temperature in the transmission geometry using a constant acceleration type spectrometer in the velocity range from $-v_{max}$ to v_{max} (from −10 to 10 mm/s and from −5 to 5 mm/s) using Fe^{57} as a source. The spectra were folded and analysed using the least-squares Mössbauer fitting program MOS.

3. Results and discussion

X-ray diffraction measurement identified rhombohedral $Na_3Fe_2P_3O_{12}$ as the main phase, rhombohedral Fe_2O_3 and patterns belonging to nonstoichiometric sodium and zirconium phosphates: $NaZr_{1.88}P_3O_{12}$, $Na_2ZrP_2O_8$ or $Na_{5-4x}Zr_{1+x}(PO_4)_3$ in material sintered in air (Fig. 1a). The multiphase product containing trivalent iron (red color of sample A, insert Fig. 1a) was always obtained after sintering in air.

The X-ray diffraction of material sintered in the conditions of reduced oxygen pressure (sample B) was found to be single phase (grey color) and free from detectable iron (e.g. Fe_3O_4) or zirconium (e.g. ZrO_2, $NaZr_{1.88}(PO_4)_3$) impurities (Fig. 1b). This phase was isomorphous with $Na_3Fe_2P_3O_{12}$. The unit cell parameters of $Na_3Zr_{1-y}Fe_{1-y}{}^{+2}Fe_{2y}{}^{+3}P_3O_{12}$ were calculated using Rietveld method by fitting X-ray diffraction data with

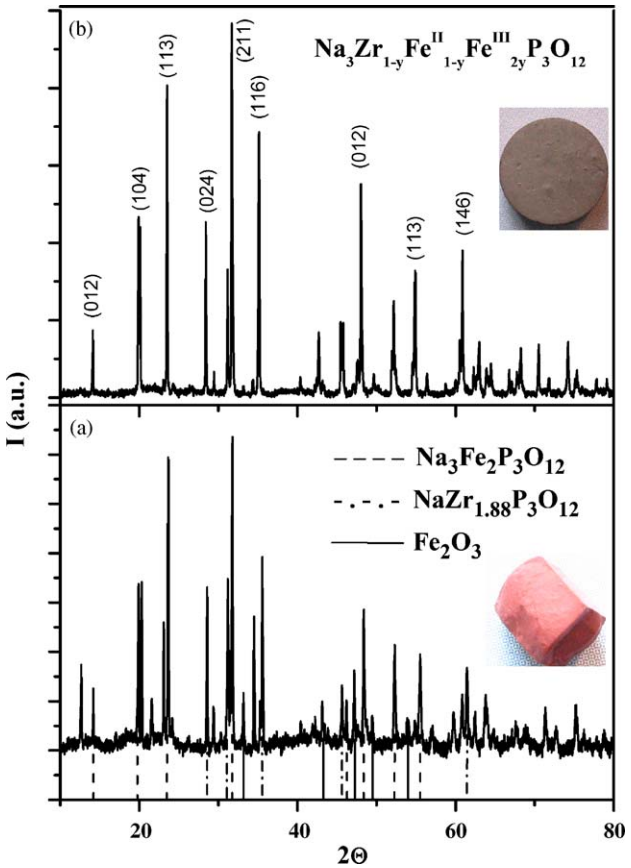

Fig. 1. X-ray diffraction pattern of material sintered in air (a) and reduced oxygen partial pressure (b).

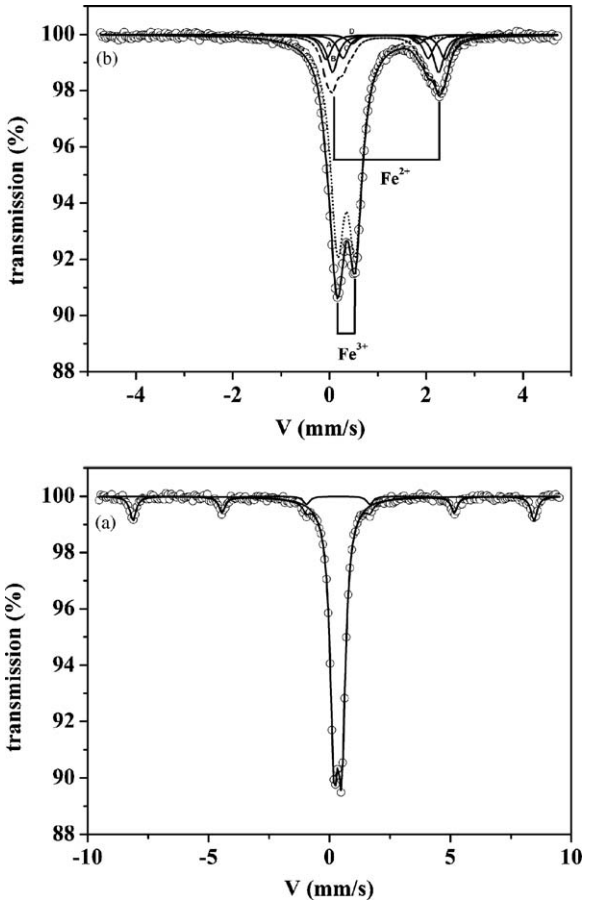

Fig. 2. Mössbauer effect spectra of material sintered in air (a) and reduced oxygen partial pressure (b).

literature data for rhombohedral (space group $R\bar{3}c$ (167)) γ-$Na_3Fe_2P_3O_{12}$ (ICSD 89991) [9–14,19]. The calculated lattice constants of $Na_3Zr_{1-y}Fe^{2+}{}_{1-y}Fe^{3+}{}_{2y}P_3O_{12}$ showed higher values ($a = 0.8848$ nm, $c = 2.1997$ nm) in comparison with γ-$Na_3Fe_2P_3O_{12}$ ($a = 0.8727$ nm, $c = 2.1807$ nm), as the result of the partial replacement of the smaller Fe^{3+} ions by bigger Fe^{2+} and Zr^{4+} ($2\ Fe^{3+} = Fe^{2+} + Zr^{4+}$) in the $Na_3Fe_2P_3O_{12}$ framework. These results were confirmed by the following Mössbauer effect studies.

The room temperature Mössbauer spectrum of the product obtained after calcinations in reducing atmosphere is shown in Fig. 2b. In order to compare the difference in the shape of spectra and Mössbauer parameters the results for sample A are also included (Fig. 2a). The velocity was estimated experimentally. For sample B below −4 and above 4 mm/s any changes in transmission were detected in contrast to sample A. The experimental data (black circles) were fitted using program MOS.

The doublet corresponding to Fe^{3+} (dotted line) and the summarized component of Fe^{2+} (dashed line) form the theoretical spectrum, which is drawn in solid line (Fig. 2b). The deconvolution of Fe^{2+} signal into four peaks (solid lines A, B, C, and D) is also shown in Fig. 2b. Mössbauer parameters for samples A and B are presented in Table 1.

Mössbauer spectrum of the multiphase product containing different Fe^{3+} compounds (sample A) is shown in Fig. 2a. The quadruple doublet corresponds to the high spin Fe^{3+} ions in octahedral coordination. The shape of spectra is similar like obtained for the different NASICON-type compounds containing trivalent iron [6,7,18]. In addition, sample A shows sextet characteristic of Fe_2O_3 phase. We may observe six magnetic splitting signals because iron nucleus can exist in six equal positions. All Fe^{3+} ions in Fe_2O_3 are in octahedral coordination [16,17]. This phase is also detected by X-ray diffraction (Fig. 1a). The similar spectrum, composed by Fe^{3+} signals from two different phases (in phosphate and oxide) was presented earlier for $Fe_xNbTiP_3O_{12}$ [8].

$Na_3Zr_{1-y}Fe^{2+}{}_{1-y}Fe^{3+}{}_{2y}P_3O_{12}$ (Fig. 2b) shows an asymmetric Mössbauer spectrum, which can be fitted by two quadrupolar split components corresponding to divalent and trivalent iron. This indicates on the incomplete reduction of Fe^{3+} to Fe^{2+}. The large values of quadrupolar split and isomer shift are referred to the Fe^{2+} in high-spin octahedral configuration, while smaller values are characteristic for trivalent iron in octahedral sites (Table 1). In addition, the presence of FeO_6 and ZrO_6 (which the cations may be Fe^{2+}, Fe^{3+} and Zr^{4+}) octahedra around the Fe^{2+} species causes the displacement of Fe^{2+} ions from the regular octahedral coordination and is reflected by components C-D on the Mössbauer spectrum (Fig. 2b). Quadrupolar splittings of C and D components are smaller in comparison with to A, B. The change of distortion of the coordinated polyhedra around the divalent iron causes an increase of the lattice contribution to the electric-field gradient, resulting in smaller quadrupolar splittings. The similar values of isomeric shift for Fe^{3+} in both $Na_3Zr_{1-y}Fe_{1-y}{}^{2+}Fe_{2y}{}^{3+}P_3O_{12}$ and samples A (Table 1) indicate on the presence of a very symmetrical Fe^{3+} octahedra, without a significant influence of surrounding charges (Zr^{4+}, Fe^{3+}). The

Table 1
Isomer shift (IS), quadruple splitting (QS), effective superfine field (H) obtained from experimental data and results presented by others.

$Na_3Zr_{1-y}Fe_{1-y}{}^{2+}Fe_{2y}{}^{3+}P_3O_{12}$

	S	γ (%)	IS(mm/s)	QS(mm/s)	IS [ref.]	QS [ref.]
Fe^{2+}	0.2335	26.9	1.1596	1.038	0.91 [7]	1.84 [7]
Fe^{3+}	0.6333	73.1	0.3499	0.1849	0.33 [7]	0.19 [7]

$Na_3Fe_2P_3O_{12}$–Fe_2O_3–$Na_2Zr(PO_4)_2$–$NaZr_{1.88}(PO_4)_3$–$Na_{5-4x}Zr_{1+x}(PO_4)_3$

	S	γ Fe^{3+}(%)	IS(mm/s)	QS(mm/s)	H(kGs)	IS [ref.]	QS [ref]	H [ref.]
$Na_3Fe_2P_3O_{12}$	0.8506	86.1	0.3445	0.1571	–	0.45 [18]	0.31 [18]	–
Fe_2O_3	0.1370	13.9	0.260	−0.096	513.8	0.37 [17]	0.22 [17]	517.5 [17]

higher value of the Fe^{2+} isomer shift for sample B in comparison with the same parameter detected for Fe_xNb-TiP_3O_{12} may be associated with its longer iron-oxygen distances [8]. However, additional investigations are required for this hypothesis. The isomeric shift and quadrupolar splitting of the Fe^{3+} component are similar to those obtained for $Ca_{0.5}H_xNbFe_{1-x}Fe_x(PO_4)_3$ [7]. In addition, the value of Fe^{2+} isomeric shift observed in our experiment is comparable to the same parameter for $Ca_{0.5}H_xNbFe_{1-x}Fe_x(PO_4)_3$, but the quadruple splitting of Fe^{2+} is lower than reported in work [7].

The isomer shift and quadrupolar splitting calculated for Fe^{3+} in sample A are lower than the same parameters presented for α-$Na_3Fe_2P_3O_{12}$ [18]. This suggests more symmetrical FeO_6 octahedra in the γ-$Na_3Fe_2P_3O_{12}$ framework (the main phase obtained after sintering in air, sample A) and can be explained as the effect of different crystallographic structure (α-$Na_3Fe_2P_3O_{12}$ is monoclinic, space group C2/*c* [6]). The different crystal symmetries are due to the changes in the distribution of alkali cations within the $Fe_2(PO_4)_3$ ribbons. In this case, the influence of Na occupations on the symmetry of polyhedra should be expected [18].

The molar amount of iron is calculated from the integrated areas under Fe^{2+} and Fe^{3+} peaks (Fig. 2b) according to the following formula [15]:

$$\gamma_{Fe^{2+}} = \frac{f_{Fe^{2+}} \cdot S_{Fe^{2+}}}{f_{Fe^{2+}} \cdot S_{Fe^{2+}} + f_{Fe^{3+}} \cdot S_{Fe^{3+}}} \quad \text{and} \quad \gamma_{Fe^{3+}} = 1 - \gamma_{Fe^{2+}},$$

where: $S_{Fe^{2+}}$, $S_{Fe^{3+}}$ area under peaks, $f_{Fe^{2+}}$, $f_{Fe^{3+}}$ recoil-free fractions ($f_{Fe^{2+}} \approx f_{Fe^{3+}}$ at room temperature).

The molar contents of Fe^{2+} and Fe^{3+} ions are 0.269 and 0.731, respectively and are slightly higher than assumed (Fe^{2+}/Fe^{3+} = 1/2). Taking into account an experimentally estimated amount of iron in $Na_3Zr_{1-y}Fe_{1-y}{}^{2+}Fe_{2y}{}^{3+}P_3O_{12}$ the electroneutrality condition would not be fulfilled as the result of an extended negative charge (∼0.345 mol) in the oxygen sublattice. In such case the calculation error (e.g. from the factorization of Mössbauer spectra) must be considered. We did not find any additional crystalline phase by XRD (Fig. 1b) and from SEM observations (data no shown), which could appear to balance the charges during synthesis of $Na_3Zr_{1-y}Fe_{1-y}{}^{2+}Fe_{2y}{}^{3+}P_3O_{12}$.

4. Conclusions

In this work, it was demonstrated that the NASICON containing both Fe^{3+} and Fe^{2+} in the lattice could be obtained by co-precipitation method and in appropriate sintering conditions. X-ray diffraction results, confirmed by the Mössbauer effect measurements showed the presence of single NASICON phase, which was isostructural with γ-$Na_3Fe_2P_3O_{12}$. The calculated unit cell parameters of NASICON indicated on the partial replacement of trivalent iron by Zr^{4+} and Fe^{2+} in $Na_3Fe_2P_3O_{12}$ framework and the formation of $Na_3Zr_{1-y}Fe_{1-y}{}^{2+}Fe_{2y}{}^{3+}P_3O_{12}$. The sintering in air led to the multiphase product with different Fe^{3+} compounds. The Mössbauer spectroscopy was applied for the first time to investigate metal incorporation in $Na_3Zr_{1-y}Fe_{1-y}{}^{2+}Fe_{2y}{}^{3+}P_3O_{12}$ lattice. From the comparison of the shape of spectrum and values of Mössbauer parameters with results presented by others for similar compounds, it was possible to describe surroundings and the position of iron in the NASICON framework. The Mössbauer spectroscopy can be used for the quantitative analysis of the Fe-modified NASICONs.

Acknowledgements

We would like to express our thanks to Dr. Mirosław Bućko and Dr. Janusz Przewoźnik for measurements and help in interpretation of data. The financial support of Polish State Committee for Scientific Research (KBN), Project No. 3T08D 01428 is acknowledged.

References

[1] P. Pasierb, Application of NASICON and YSZ for the construction of CO_2 and SO_x potentiometric gas sensors, Material Science 24 (1) (2006) 279–284.
[2] E. Siebert, P. Fabry, NASICON type ionic conductors for alkali ion sensing, Ionics 5 (3/4) (1999) 261–268.
[3] S. Yde-Andersen, J.S. Lundsgaard, L. Moeller, J. Engell, Properties of Nasicon electrolytes prepared from alkoxide derived gels: ionic conductivity, durability in molten sodium and strength test data, Solid State Ionics 14 (1) (1984) 73–79.
[4] H.Y-P. Hong, Crystal structures and crystal chemistry in the system $Na_{1+x}Zr_2Si_xP_{3-x}O_{12}$, Materials Research Bulletin 11 (1976) 173–182.
[5] H. Kageyama, N. Kamijo, T. Asai, Y. Saito, K. Ado, O. Nakamura, XAFS study of NASICON-related compounds, sodium zirconium cobalt iron phosphate ($Na_3Zr_{0.5}Co_{0.5}FeP_3O_{12}$) and sodium zirconium iron phosphate ($Na_3Zr_{0.5}Fe^{(II)}{}_{0.5}Fe^{(III)}P_3O_{12}$), Solid State Ionics 40/41 (1990) 350–356.
[6] A.S. Andersson, B. Kalska, P. Eyob, D. Aernout, L. Haggstrom, J.O. Thomas, Lithium insertion into rhombohedral $Li_3Fe_2P_3O_{12}$, Solid State Ionics 140 (2001) 63–70.
[7] B. Srinivasulu, M. Vithal, Preparation of a new family of NASICON type phosphates $Ca_{0.5}NbMP_3O_{12}$ (M = Fe, Al, Ga and In) and characterization of the iron systems by Mössbauer spectroscopy, Journal of Materials Science Letters 18 (1999) 1771–1773.
[8] F.J. Berry, R. Gancedo, J.F. Marco, R.C. Thied, Mössbauer spectroscopic investigation of metal incorporation within NASICON-related $NbTiP_3O_{12}$, Journal of the Chemical Society – Dalton Transactions (1994) 1703–1710.
[9] T. Asai, K. Ado, Y. Saito, H. Kegayama, O. Nakamura, Mixed conductivity of $Na_{1+4x}M_x{}^{II}Fe_{2-x}{}^{III}Zr_{2-3x}P_3O_{12}$,$M^{II}$:iron$^{(2+)}$, cobalt$^{(2+)}$ and nickel$^{(2+)}$, Solid State Ionics 35 (1989) 319–322.
[10] O. Tillement, J. Angenault, J.C. Couturier, M. Quarton, Mixed conductivity of the NASICON phase sodium zirconium iron phosphate ($Na_{2+x+-y}Zr_{1-y}Fe_x{}^{II}Fe_{1-x+y}{}^{III}(PO_4)_3$), Solid State Ionics 44 (1991) 299–303.
[11] G. Rousse, J. Rodriguez-Carvajal, C. Wurm, C. Mascquelier, Magnetic structure of two lithium iron phosphates: A- and B-$Li_3Fe_2(PO_4)_3$, Applied Physics A 74 (2002) S704–S706.
[12] M. Catti, A Mixed α/β Superstructure in NASICON Ionic Conductors: neutron diffraction study of $Li_2FeTi(PO_4)_3$ and $Li_2FeZr(PO_4)_3$, Journal of Solid State Chemistry 156 (2001) 305–312.
[13] F. d'Yvoire, M. Pintard-Screpel, E. Bretey, M. De la Rochere, Phase transitions and ionic conduction in 3D skeleton phosphates $A_3M_2(PO_4)_3$: A = Li, Na, Ag, K; M = Cr, Fe, Solid State Ionics 9 & 10 (1983) 851–858.
[14] C. Masquelier, C. Wurm, J. Rodriguez-Carvajal, J. Gaubicher, L. Nazar, A powder neutron diffraction investigation of the two rhombohedral NASICON analogues: γ-$Na_3Fe_2(PO_4)_3$ and $Li_3Fe_2(PO_4)_3$, Chemistry of Materials 12 (2000) 525–532.
[15] C.A. McCammon, The crystal chemistry of ferric iron in $Fe_{0.05}Mg_{0.95}SiO_3$ perovskite as determined by Mössbauer spectroscopy in the tem-

perature range 80–293 K, Physics and Chemistry of Minerals 25 (1998) 292–300.

[16] M.J. Graham, D.A. Channing, G.A. Swallow, R.D. Jones, Mössbauer study of the reduction of hematite in hydrogen at 535.deg., Journal of Materials Science 10 (1975) 1175–1181.

[17] I.V. Murin, V.M. Smirnov, G.P. Voronkov, V.G. Semenov, V.G. Povarov, B.M. Sinelnikov, Structural-chemical transformations of α-Fe_2O_3 upon transport reduction, Solid State Ionics 133 (2000) 203–210.

[18] D. Beltrán-Porter, R. Olazcuaga, L. Fournes, F. Menil, G. Le Flem, Magnetic and Mössbauer resonance study of orthophosphate sodium iron phosphate α-$(Na_3Fe_2(PO_4)_3)$ and a formed vitreous phase, Revue De Physique Appliquée 15 (1980) 1155–1160.

[19] G. Rousse, J. Rodriguez-Carvajal, C. Wurm, C. Mascquelier, Magnetic structural studies of the two polymorphs of $Li_3Fe_2(PO_4)_3$: analysis of the magnetic ground state from super-super exchange interactions, Chemical Materials 13 (2001) 4527–4536.